CMTC-484390-MS

A Systematic Reservoir Simulation Study on Assessing the Feasibility of CO2 Sequestration in Shale Gas Reservoirs with Potential Enhanced Gas Recovery

Jie Zhan, University of Calgary; Qingwang Yuan, University of Regina; Allan Fogwill, Canadian Energy Research Institute; Hua Cai, CNOOC Ltd.-Shanghai; Hossein Hejazi, Zhangxin Chen, University of Calgary; Shiqing Cheng, China University of Petroleum-Beijing

This paper was prepared for presentation at the Carbon Management Technology Conference held in Houston, Texas, USA, 17-20 July 2017.

Abstract

The application of horizontal well drilling coupled with the multistage fracturing technology enables commercial development of shale gas formations, which launches the energy revolution from conventional resources to unconventional resources. With the progress of understanding the nature of shale reservoirs, we find that some shale methane is stored as an adsorbed phase on surfaces of organic carbon. Meanwhile, laboratory and theoretical calculations indicate that organic-rich shale adsorbs CO2 preferentially over CH4. Shale gas reservoirs are recently becoming the promising underground target for CO2 sequestration. In the paper, systematic numerical simulations will be implemented to investigate the feasibility of CO2 sequestration in shale gas reservoirs and quantify the associated uncertainties.

First, a multi-continua porous medium model will be set up to present the matrix, nature fractures and hydraulic fractures in shale gas reservoirs. Based on this model, we will investigate a three-stage flow mechanism which includes convective gas flow mainly in fractures, dispersive gas transport in macro pores and multi-component sorption phenomenon in micro pores. To deal with this complicated three-stage flow mechanism simultaneously, analytical apparent permeability which includes slip flow and Knudsen diffusion will be incorporated into a commercial simulator CMG-GEM. A Langmuir isotherm model is used for CH4 and the multilayer sorption gas model, a BET model, is implemented for CO2. In addition, a mixing rule is introduced to deal with the CH4-CO2 competitive adsorption phenomenon.

In the paper, an integrated methodology is provided to investigate the CO2 sequestration process. Simulation results indicate that a shale gas reservoir is an ideal target for the CO2 sequestration. Even with the reservoir pressure maintenance due to the injection of CO2, the reservoir productivity is not enhanced. Hydraulic fracking which creates freeways for gas flow is the key to improve the reservoir

performance. The multicomponent desorption/adsorption is a very important feature in a shale gas reservoir, which should be fully harnessed to benefit the CO2 sequestration process. In addition, we cannot ignore the contribution of slip flow and diffusion to the reservoir performance. Based on the methodology provided in this paper, we can easily deal with the apparent permeability effect using a commercial simulator platform.

Introduction

As of August 2013, the Geological Survey of Canada estimated that Canada has approximately 4,995 trillion cubic feet (Tcf) of shale gas in place, a large portion of which is located in the Western Sedimentary Basin.[1] Shale gas resources can be found in British Columbia, Alberta, Saskatchewan, Manitoba, Ontario, Quebec, New Brunswick, Nova Scotia, the Northwest Territories, and Yukon.[2] However, gas-in-place estimates are available for certain provinces only, as shown in the following figure.

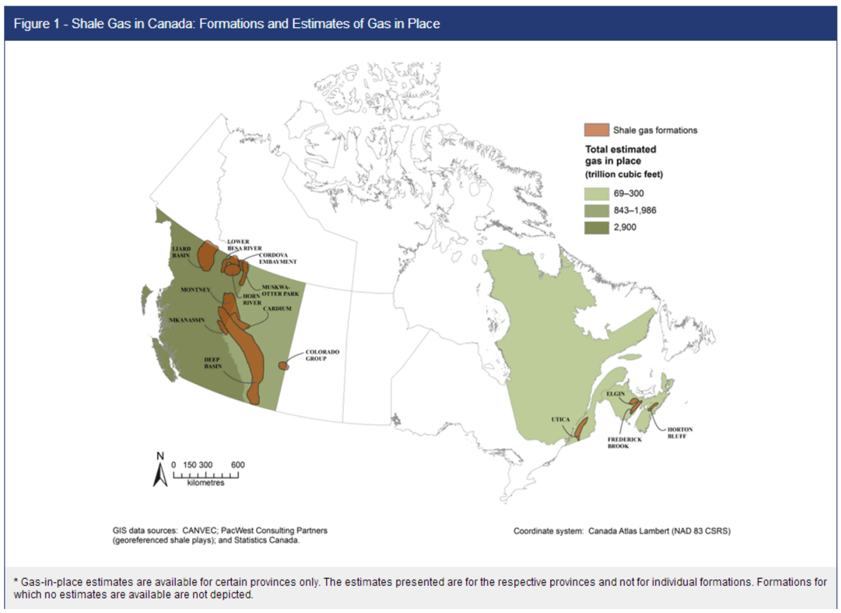

Fig. 1. Shale gas in Canada: formations and estimates of gas in place (Parliament of Canada)

The U.S. Energy Information Administration estimates that 573 Tcf of Canadian shale gas is technically recoverable, which represents nearly 8% of the global estimated total. According to this assessment, Canada has the world's fifth largest shale gas deposit, after China (1,115 Tcf), Argentina (802 Tcf), Algeria (707 Tcf) and the U.S. (665 Tcf).[3]

Composed principally of methane (CH4), natural gas produces far fewer potentially hazardous pollutants than coal when combusted. It also produces 43% fewer carbon dioxide (CO_2) emissions per unit of produced energy than coal. Used for electricity generation, a combined cycle gas turbine power plant can achieve typical efficiencies greater than 50%.[4] These environmental factors, combined with changes in natural gas markets, have led to the percentage of electricity supplied by natural gas nearly doubling over the last 20 years in the United States, increasing from 11.9% of electricity in 1989 to 23.2% in 2009.[5] Similar trends can be observed globally, where annual natural gas consumption is expected to increase from 108 Tcf in 2007 to 156 Tcf in 2035. Compared with its southern neighbor (U.S.), Canada's shale gas production is still in its early stages and production activities concentrate primarily in western Canada. For Canada, a rise in shale gas production at home and abroad could mean unprecedented economic opportunities and future prosperity.[6]

With the progress of understanding the nature of shale reservoirs, we find that some shale methane is stored as an adsorbed phase on the surfaces of organic carbon. Meanwhile, laboratory and theoretical calculations indicate that organic-rich shale adsorbs CO_2 preferentially over CH_4. With the help of CO_2 tax and the generation of an income stream through potential enhanced recovery of shale gas which recoups some of the cost of capturing and sequestering CO_2, shale gas reservoirs become the most economically promising underground target for CO_2 sequestration.[7,8] Moreover, with the high well density in shale gas fields, additional wells may not need to be drilled to implement enhanced recovery, further reducing the cost of sequestration. But there are many challenges to prove the viability of sequestration and enhanced recovery in gas shale because the performance of CO_2 injection in shale reservoirs is influenced by several engineering parameters.[9] Based on a sophisticated shale gas reservoir model which includes multi-continua, a three-stage flow mechanism and multi-component sorption, a systematic numerical simulation study will be implemented to assess the feasibility of the CO_2 sequestration process and quantify its uncertainties.

Numerical simulation methods

We use CMG-GEM, the advanced general EOS compositional reservoir simulator, to model multiple hydraulic fractures and gas flow in shale reservoirs.[10] In the simulation model, we assumed that gas is flowing into a wellbore through hydraulic fractures with considering a non-Darcy effect. We implement the correlation proposed by Evan and Civan to determine the non-Darcy beta factor which is used in the Forchheimer number.[11,19,20] Local grid refinement with logarithmic spacing is employed to accurately simulate the detailed transient gas flow phenomenon around hydraulic fractures. A dual-permeability model is used to take natural fractures into consideration. The logarithmically spaced, locally refined, dual permeability (LS-LR-DK) methodology has been widely applied to model gas flow in hydraulically fractured shale gas reservoirs.[12, 13, 14] Grid blocks which include hydraulic fractures have a $7 \times 7 \times 1$ local grid refinement. The refined blocks along the center of a parent block have a width of 2 ft. The hydraulic fractures are represented by these center blocks. Since a larger width (2 ft) is used for the hydraulic fracture, we need to convert the fracture conductivity in a 2 ft wide grid block. The effective permeability is calculated based on the following equation [10]:

$$K_{eff} = \frac{K_f W_f}{W_{grid}}. \quad (1)$$

where K_{eff} is the effective permeability and W_{grid} is the width of an inner grid block. In the present case, W_{grid} is 2 ft. K_f is the intrinsic permeability of fractures and W_f is the width of fractures.

Because of an increased cross-sectional area from using a larger block width, the actual velocity in the fractures is higher than the velocity in the blocks. Therefore, a non-Darcy correction coefficient is defined so that flow resistance arising from the non-Darcy effect is correctly captured: [10]

$$\beta_{corr} = \left(\frac{K_f}{K_{eff}}\right)^{2-N_{1g}} = \left(\frac{W_{grid}}{W_f}\right)^{2-N_{1g}}. \quad (2)$$

where β_{corr} is the non-Darcy correction factor and N_{1g} is the first coefficient in the Forchheimer equation for non-Darcy flow.

In addition, CH_4 adsorption on solid surfaces is taken into consideration in the model through implementing the classical Langmuir isotherm.[15] The Langmuir isotherm equation with two fitting parameters is as follows:

$$V(P) = \frac{V_L \mathrm{P}}{P+P_L}, \tag{3}$$

where $V(P)$ is the gas volume of adsorption at pressure P, V_L is the Langmuir volume, referred to the maximum adsorbed gas volume at the infinite pressure, and P_L is the Langmuir pressure which represents the pressure corresponding to a one-half Langmuir volume.

The multilayer sorption gas model, [16] a general BET model, is implemented for CO_2. The general BET model with the four fitting parameters is as follows:

$$V(P) = \frac{V_m C \frac{P}{P_0}}{1-\frac{P}{P_0}} \left[\frac{1-(N+1)\left(\frac{P}{P_0}\right)^N + N\left(\frac{P}{P_0}\right)^{N+1}}{1+(C-1)\frac{P}{P_0} - C\left(\frac{P}{P_0}\right)^{N+1}} \right]$$

where P_0 is the saturation pressure of gas, V_m is the maximum adsorption gas volume when the entire adsorbent surface is covered with a unimolecular layer, C is a constant related to the net heat of adsorption, and N is the maximum number of adsorption layers.

In the model, an extended Langmuir isotherm is implemented to model the competitive multicomponent adsorption and desorption process:[10]

$$wi = \frac{w_{i,max} B_i y_{ig} P}{1+\sum_j B_j y_{jg}}$$

where w_i is the moles of adsorbed component i per unit mass or rock, $w_{i,max}$ is the maximum moles of adsorbed component i per unit mass or rock, Bi is the parameter for Langmuir isotherm relation, P is the pressure, and y_{ig} is the molar fraction of adsorbed component i in the gas phase.

The transport mechanism of shale gas in matrix pores devidates from the conventional Darcy flow equation, as shown in the following Fig. 1. [17]

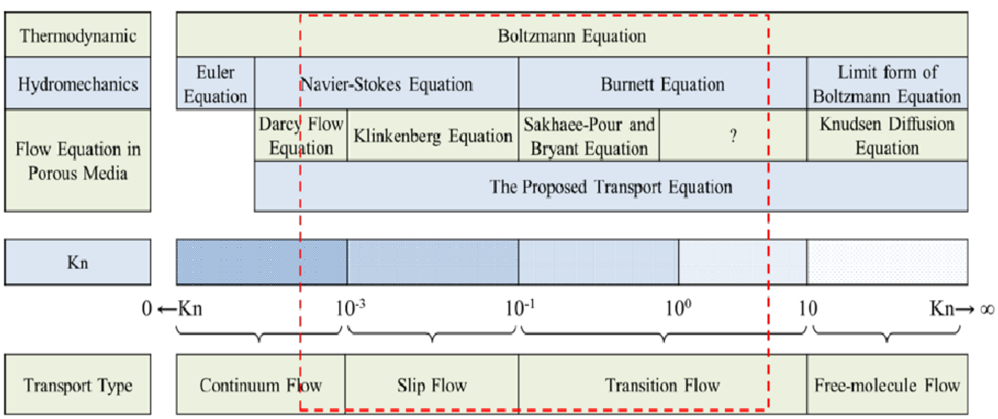

Fig. 1. Gas flow regimes divided by Kn (Dr. J. Shi)

Apparent permeability which combines slip flow and Knudsen diffusion will be incorperated into the shale gas reservoir model, [18]

$$k = \left[\sqrt{\frac{8RT}{\pi M}} \left(\frac{2}{3RT\,\rho_{avg}} + \frac{\pi}{8P_{avg}} \left(\frac{2}{\alpha} - 1 \right) \right) r\mu + \frac{r^2}{8} \right]$$

We assume that the average radius of a nano matrix pore is 2 nm. Based on the above equation, we can plot the relationship between the apparent permeability and the reservoir pressure. With a decrease in the reservoir pressure, the apprarent permeability will increase. That is also the reseason that we can see the more-than-expected gas production from a shale gas reservoir.

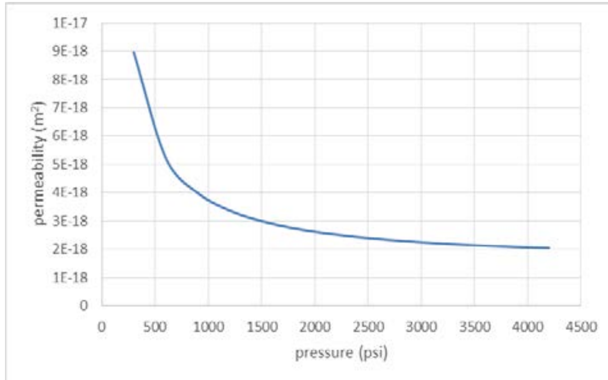

Fig. 2. The relationship between the apparent permeability and the reservoir pressure

Here is the ratio of the apparent permeability over the Darcy permeability, which will be integrated into the commercial simulator CMG-GEM to examine the effect of the transport mechanism on the CO_2 sequestration process.

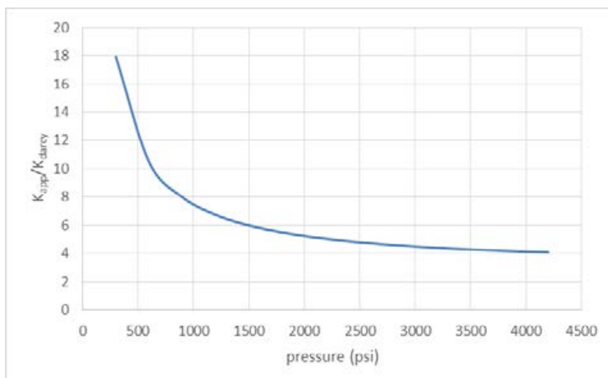

Fig. 3. The ratio of apparent permeability over the darcy permeability versus the pressure

Reservoir model

A shale reservoir is simulated by setting up a homogeneous 3D reservoir model with dimensions of $5000ft \times 3000ft \times 300ft$, which correspond to the length, width and thickness, respectively (Fig. 4). A horizontal well with ten fracturing stages is simulated. The hydraulic fracture spacing and the half-length are 450 ft and 425 ft, respectively. The spacing between the two horizontal wells is 1000 ft. The detailed information of the reservoir and hydraulic fractures is listed in Table 1. The adsorption data and relative permeability data for each domain (matrix, hydraulic fractures and natural fractures) are listed in Table 2. The overall production period is 30 years. First of all, well-1 and well-2 are set to produce for five years. Then well-2 is converted to an injection well (well-3) with the injection rate of 1×10^6 ft^3/day. The injection time is 5 years.

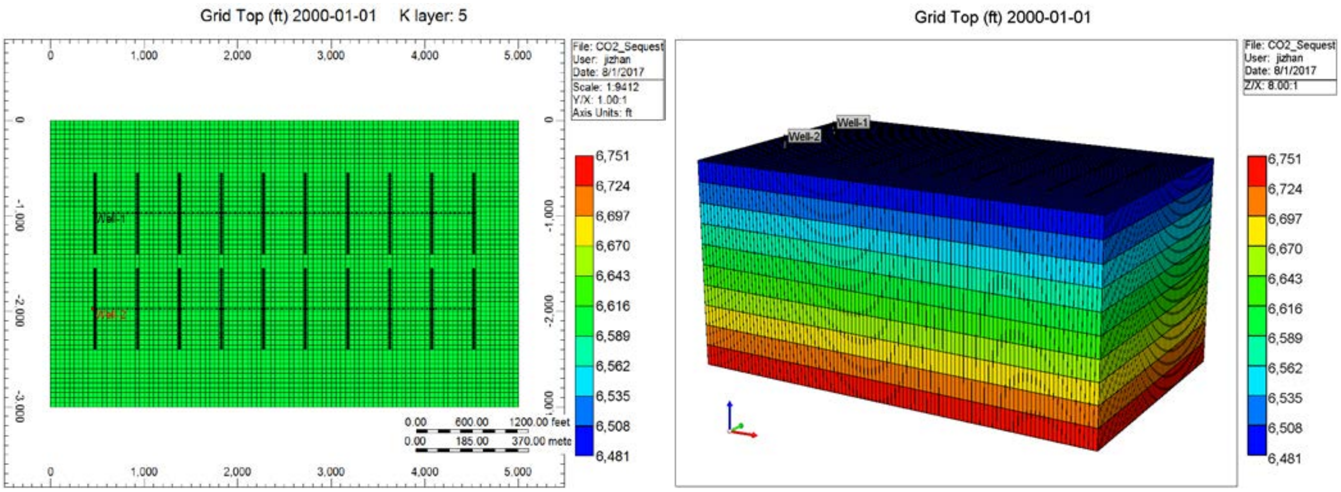

(a) 2D view (b) 3D view

Fig. 4. Shale gas reservoir model

Table 1: Parameters used in the shale gas reservoir model

Parameter	Value(s)	Unit
The model dimensions	5000×3000×300	ft
Grid Top Depth	6481	ft
Pore pressure gradient	0.54	psi/ft
STG	2000000	ft^3/day
BHP	300	psi
Production time	30	year
Reservoir Temperature	150	F
Initial gas saturation	0.8	
Total compressibility	1.E-06	psi^{-1}
Matrix permeability	0.0005	md
Matrix porosity	0.06	
Fracture permeability	2.E-05	md
Fracture porosity	4.E-05	
Fracture Conductivity	10	md*ft

Table 2: Adsorption data and relative permeability data for different continuum

	Matrix	HF	NF
Adsorption Data	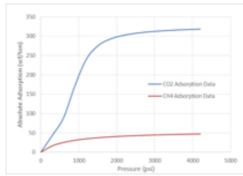	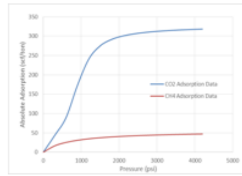	**No Adsorption**
Relative Perm	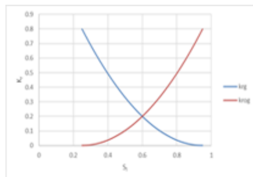	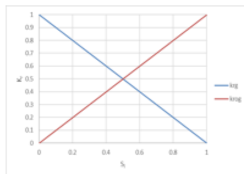	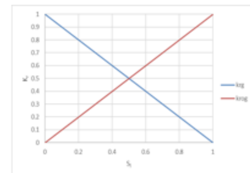

As shown in the following figures, 99% of the injected CO_2 has been sequestered successfully in the Barnett shale formation for one horizontal well in a 30-year period.

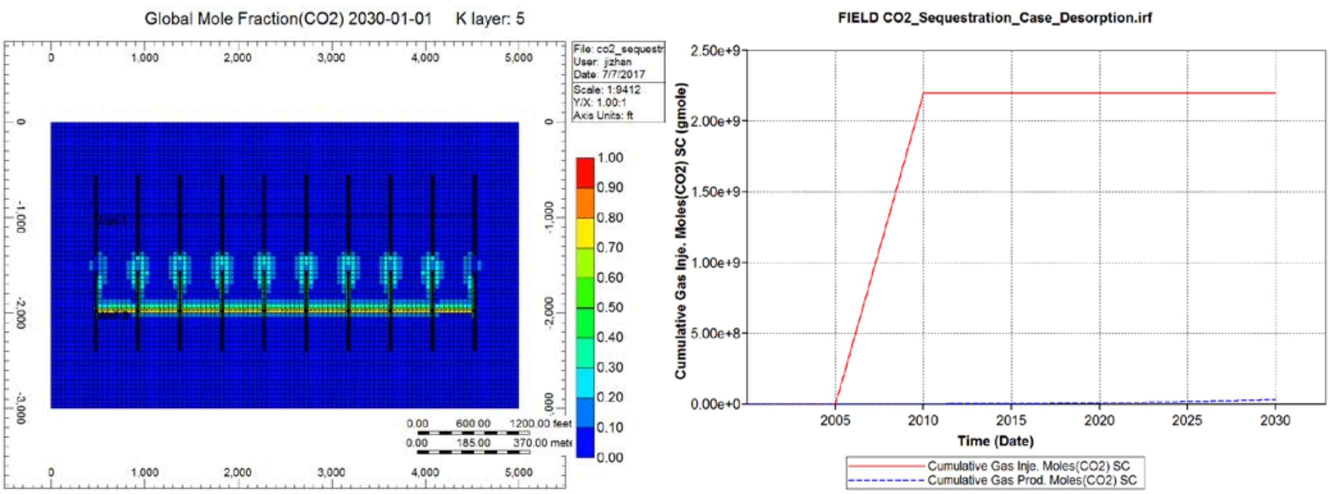

(a) CO_2 mole fraction distribution (b) Cumulative CO_2 injection and production

Fig. 5. Simulation results on the CO2 sequestration for the Darcy permeability case

Due to the CO_2 injection, the reservoir pressure is maintained. But the final CH_4 recovery is the same for the two cases because of the limitations of the tight formation. Meanwhile, we can observe that the adsorption/desorption process makes contribution to the reservoir pressure maintenance and reservoir productivity, which is a very important feature of a shale gas reservoir. A shale gas reservoir is an ideal target for the CO_2 sequestration. Even with the reservoir pressure maintenance due to the injection of the CO_2, the reservoir productivity is not enhanced. Hydraulic fracking which creates freeways for gas flow is the key to improve the reservoir performance.

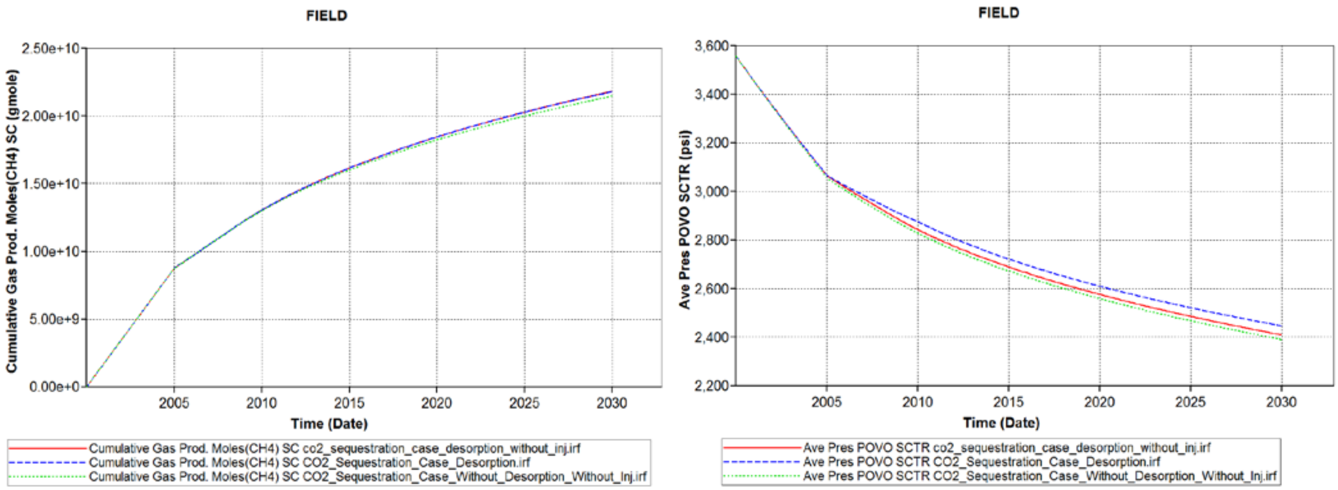

(a) Cumulative CH_4 production (b) Average reservoir pressure

Fig. 6. Simulation results on reservoir performance

Here, we will examine the effect of the three-stage flow mechanism via integrating the analytical apparent permeability model into the shale gas numerical model.

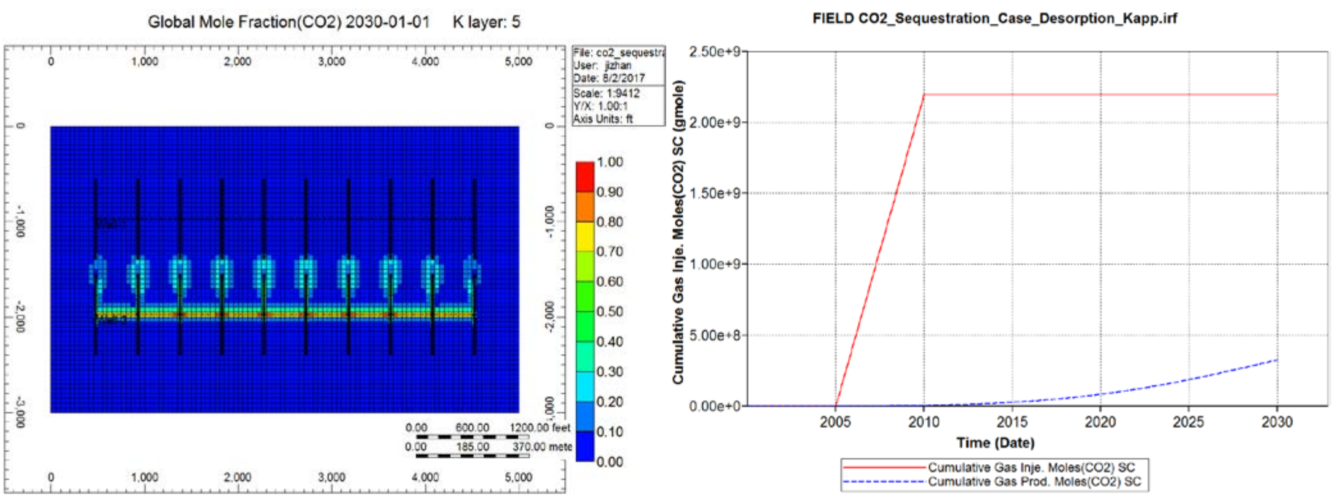

(a) CO_2 mole fraction distribution (b) Cumulative CO_2 injection and production

Fig. 7. Simulation results on the CO2 sequestration for the apparent permeability case

Just as in the following figure, we can observe that the apparent permeability is about 4 times bigger than the Darcy permeability (0.0005 md) during the 30-years production period. Due to the integration of the apparent permeability, the reservoir is more permeable. That is why more CO_2 will be produced from the reservoir. Moreover, the apparent permeability is the function of the reservoir pressure. The pressure heterogeneity will lead to the apparent permeability heterogeneity so that we can observe that the CO2 mole fraction distribution is not as uniform as in the Darcy permeability case.

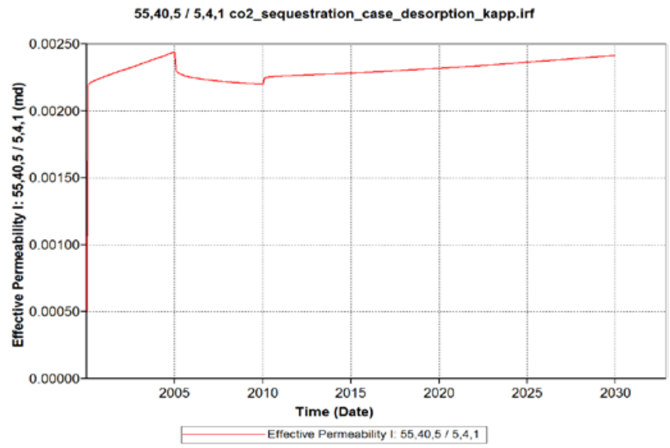

Fig. 8. Apparent permeability evolution for specific reservoir location with CO_2 injection

There is also a big difference on the average reservoir pressure and the CH_4 productivity. Due to the bigger apparent permeability, the pressure is easier to trasnsimit which leads to the bigger productivity. Based on the above analysis, the apparent permeability effect which includes slip flow and diffusion in addtion to the Darcy permeability is not negelible when we deal with a shale reservoir. The slip flow and diffusion make lots of contribution to the reservoir performace as we can observe from the cumulative CH_4 gas production.

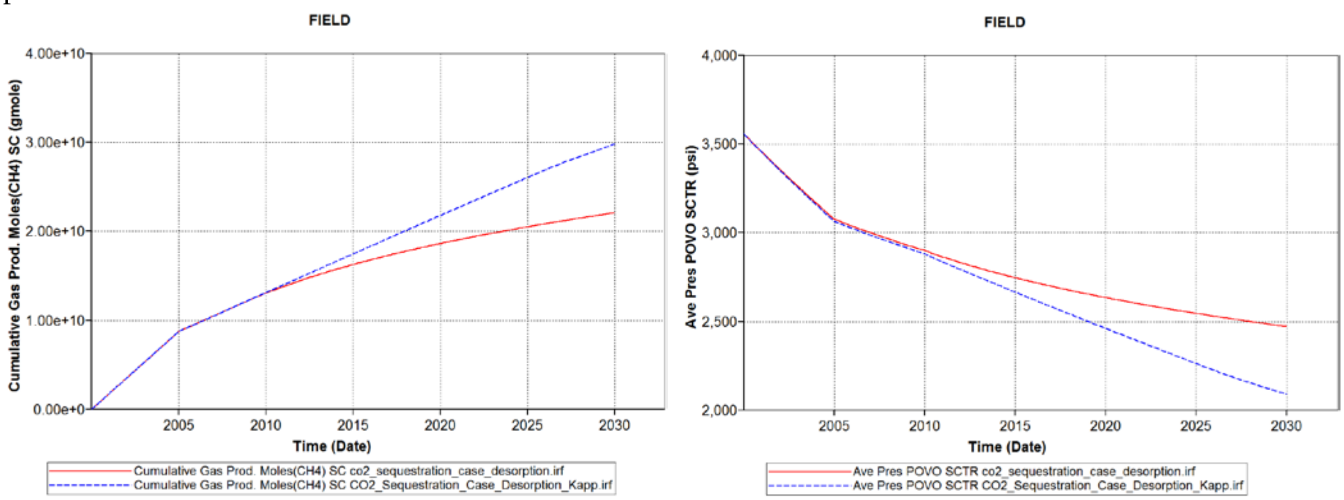

(a) Cumulative CH_4 production (b) Average reservoir pressure

Fig. 9. Reservoir performance comparison between the apparent and darcy permeability case

We can find one more interesting phenomenon with the integration of the apparent permeability model into the commerical simulator. Due to the injection process which leads to an increase in the reservoir pressure, the apparent permeability decreases with an increase in the reservoir pressure. That is why we can observe slightly bigger cumulative CH_4 production for the case without injection. It further validates the point that the permeable pathway for gas flow is the key to improve the reservoir performance at this point compared with the reservoir pressure maintenance.

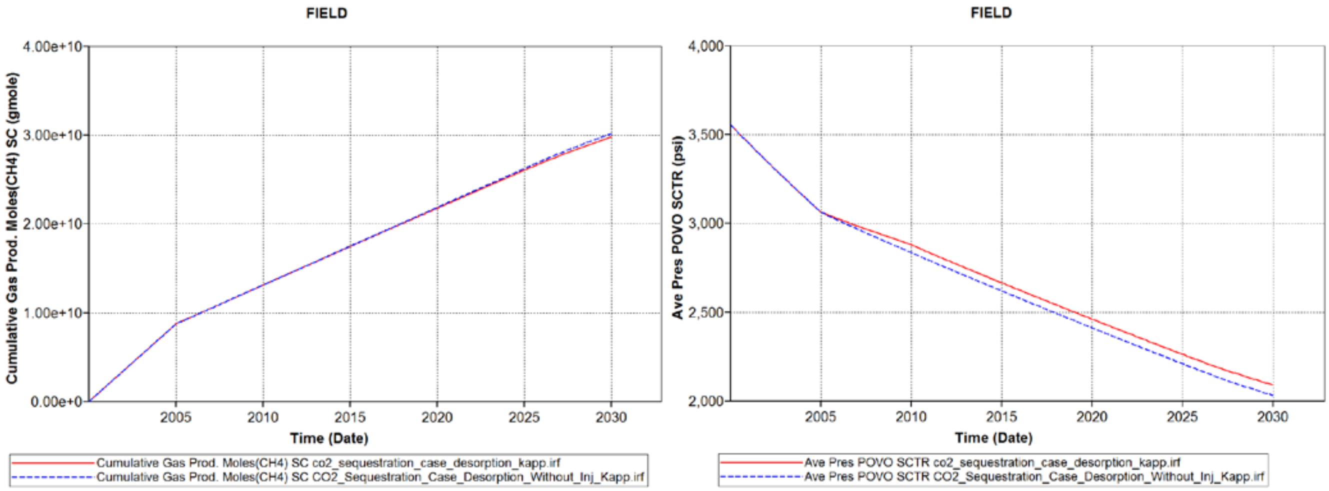

(a) Cumulative CH_4 production (b) Average reservoir pressure

Fig. 10. Simulation results on reservoir performance for the apparent permeability case

For the apparent permeability evolution, we can observe that there will be a five-year decrease for the case with injection. For the case without injection, after an immediate drop due to the well-2 shut-in, the apparent permeability will increase till the end of the simulation. That is why we can observe the above interesting phenomenon.

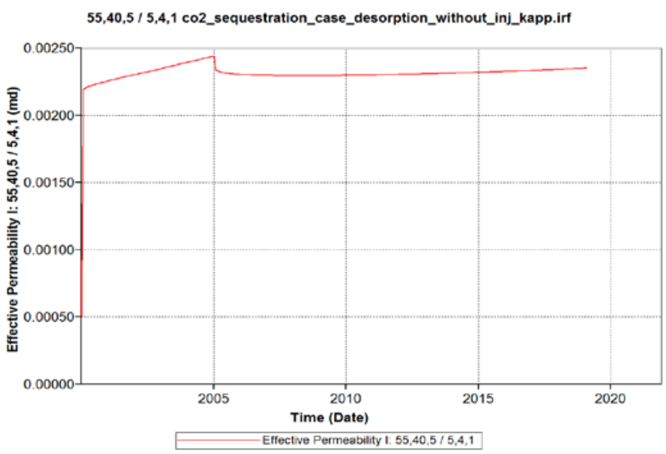

Fig. 11. Apparent permeability evolution for specific reservoir location without CO_2 injection

Conclusion and Future Work

An integrated methodology is provided to investigate the CO_2 sequestration process. A shale gas reservoir is an ideal target for the CO_2 sequestration. Even with the reservoir pressure maintenance due to the injection of CO_2, the reservoir productivity is not enhanced. Hydraulic fracking which creates freeways for gas flow is the key to improve the reservoir performance. The multicomponent desorption/adsorption is a very important feature in a shale gas reservoir, which should be fully harnessed to benefit the CO_2 sequestration process. In addition, we cannot ignore the contribution of slip flow and diffusion to the reservoir performance. Based on the methodology provided in this paper, we can easily deal with the apparent permeability effect based on a commercial simulator platform. In the near future, we will examine the stress-sensitivity effect on natural fractures in shale reservoirs via implementing the elastic geomechanics model and the Barton-Bandis model. Reservoir heterogeneity will also be taken into account in the future study. Moreover, different well operation schemes will be tested based on the integrated shale gas reservoir model. Based on the improved reservoir understanding, some economic and environmental assessments associated with production efficiency and carbon sequestration will be conducted.

Acknowledgment

The authors would like to acknowledge the support of Department of Chemical and Petroleum Engineering, University of Calgary and Canadian Energy Research Institute. The Reservoir Simulation Group is gratefully acknowledged. The research is partly supported by NSERC/AIEES/Foundation CMG, AITF iCore, IBM Thomas J. Watson Research Center, and the Frank and Sarah Meyer FCMG Collaboration Centre for Visualization and Simulation.

Reference

1. Energy and Mines Ministers' Conference (2013).

2. Understanding Shale Gas in Canada. Canadian Society for Unconventional Gas.

3. U.S. Energy Information Administration (2013).

4. NETL, 2010, Fossil Energy Cost and Performance Baseline Studies.

5. EIA, 2010b, Annual Energy Review 2009.

6. U.S. Energy Information Administration, North America leads the world in production of shale gas, Today in Energy, 23 October 2013.

7. McKinsey, 2008, Carbon Capture & Storage: Assessing the Economics.

8. McKinsey, 2009, Pathways to a Low-Carbon Economy: Version 2 of the Global Greenhouse Gas Abatement Cost Curve.

9. Yu, W., Al-Shalabi, E. W., & Sepehrnoori, K. (2014, April 1). A Sensitivity Study of Potential CO_2 Injection for Enhanced Gas Recovery in Barnett Shale Reservoirs. Society of Petroleum Engineers. doi: 10.2118/169012-MS

10. CMG, 2015.GEM User's Guide. Computer Modeling Group Ltd.

11. Evan, R.D., and Civan, F.,1994. Characterization of non-Darcy multiphase flow in petroleum bearing formation. Final report, U.S. DOE Contract No. DE-AC22-90BC14659, School of Petroleum and Geological Engineering, University of Oklahoma.

12. Rubin, B. (2010, January 1). Accurate Simulation of Non Darcy Flow in Stimulated Fractured Shale Reservoirs. Society of Petroleum Engineers. doi:10.2118/132093-MS

13. Tavassoli, S., Yu, W., Javadpour, F., & Sepehrnoori, K. (2013, November 5). Selection of Candidate Horizontal Wells and Determination of the Optimal Time of Refracturing in Barnett Shale (Johnson County). Society of Petroleum Engineers. doi:10.2118/167137-MS

14. Liu F, Ellett K, Xiao Y, et al. Assessing the feasibility of CO 2 storage in the New Albany Shale (Devonian–Mississippian) with potential enhanced gas recovery using reservoir simulation[J]. International Journal of Greenhouse Gas Control, 2013, 17: 111-126.

15. Langmuir I. The adsorption of gases on plane surfaces of glass, mica and platinum [J]. Journal of the American Chemical society, 1918, 40(9): 1361-1403.

16. Brunauer S, Emmett P H, Teller E. Adsorption of gases in multimolecular layers [J]. Journal of the American chemical society, 1938, 60(2): 309-319.

17. Shi, J., Zhang, L., Li, Y., Yu, W., He, X., Liu, et al, (2013, November 5). Diffusion and Flow Mechanisms of Shale Gas through Matrix Pores and Gas Production Forecasting. Society of Petroleum

Engineers. doi:10.2118/167226-MS
18. Shabro, V., Torres-Verdin, C., & Javadpour, F. (2011, January 1). Numerical Simulation of Shale-Gas Production: From Pore-Scale Modeling of Slip-Flow, Knudsen Diffusion, and Langmuir Desorption to Reservoir Modeling of Compressible Fluid. Society of Petroleum Engineers. doi:10.2118/144355-MS.
19. Chen, Z., G. Huan & Y. Ma (2006). Computational Methods for Multiphase Flows in Porous Media. Computational Science and Engineering Series, Vol. 2, SIAM, Philadelphia.
20. Chen, Z. (2007). Reservoir Simulation: Mathematical Techniques in Oil Recovery. CBMS-NSF Regional Conference Series in Applied Mathematics, Vol. 77, SIAM, Philadelphia.

Nomenclature

K_{eff}: Effective permeability, *mD*
K_f: Fracture permeability, *mD*
W_f: Fracture width, *ft*
W_{grid}: Block width, *ft*
β_{corr}: Non-Darcy correction factor
N_{1g}: First coefficient in the Forchheimer equation for non-darcy flow
$V(P)$: Gas volume of adsorption at pressure P, *scf/ton*
V_L: Langmuir volume, *scf/ton*
P: Pressure, *psi*
P_L: Langmuir pressure, *psi*
V_m : Maximum gas adsorption volume, *scf/ton*
C : Constant related to the net heat of adsorption
N : Maximum number of adsorption layers
W_i : Moles of adsorbed component I per unit mass or rock, *mole*
$W_{i,max}$: Maximum moles of adsorbed component *i* per unit mass or rock, *mole*
B_i : Parameter for Langmuir isotherm relation
y_{ig} : Molar fraction of adsorbed component *i* in the gas phase
r : Pore radius, *ft*
R : Universal gas constant
M : Molar mass, *lbm/mole*
P_{avg} : Average pressure, *psi*
ρ_{avg} : Average gas density, lbm/ft^3
μ : Viscosity, *cp*
α: Tangential momentum accommodation coefficient
T : Temperature, *F*